

Forces between single pairs of charged colloids in aqueous salt solutions

C. Gutsche, U. F. Keyser, K. Kegler, and F. Kremer

Institut für Experimentelle Physik I der Universität Leipzig, Germany

P. Linse

Physical Chemistry 1, Center for Chemistry and Chemical Engineering, Lund University, Sweden

(Received 16 May 2007; revised manuscript received 29 June 2007; published 25 September 2007)

Forces between *single* pairs of negatively charged micrometer-sized colloids in aqueous solutions of monovalent, divalent, or trivalent counter-ions at varying concentrations have been measured by employing optical tweezers. The experimental data have been analyzed by using the Derjaguin-Landau-Verwey-Overbeek (DLVO) theory and a numerical solution of the Poisson-Boltzmann (PB) equation. With monovalent counterions, the data are well described by the DLVO and PB theories, suggesting that the DLVO theory is adequate to describe the colloidal forces at these conditions. At higher counter-ion valence, the approximations within the two theories become evident.

DOI: [10.1103/PhysRevE.76.031403](https://doi.org/10.1103/PhysRevE.76.031403)

PACS number(s): 82.70.Dd, 87.80.Cc

I. INTRODUCTION

Colloidal dispersions possess a large number of interesting and important properties and hence find applications as coatings, aerosols, and ceramics and for separation or filter processes. The size and charge of the colloids can be varied extensively, and thus the range and strength of the intercolloidal interactions can be adjusted. This makes colloidal dispersions an excellent model system to investigate fundamental issues in condensed matter physics [1]. A long-standing issue is the electrostatic interaction among charged colloids. For instance, the screening of charged colloids by counterions is central for the understanding of liquid suspensions, the stability of colloidal dispersions, and particle aggregation. Colloidal crystals are often considered as a model system for atomic crystals, with the advantage of tunable repulsion by controlling the salt concentration [2,3]. Another important subject is the behavior of vesicles and compartment stability in life science [4–8]. The latter ones play also a role in problems of drug delivery [9] and in microfluidic devices [6–8]. Also membrane fusion is strongly controlled by electrostatic interactions, by regulating the distance between the two opposite intermediate membrane “buds,” which initiate the fusion [4].

Optical tweezers [10] are ideal tools to carry out experiments with micrometer-sized objects in materials research [11–13], biological sciences [14–16], and soft matter research [17,18]. The idea behind optical tweezers is using strongly focused laser beams to trap a small dielectric particle in its focal point. Several considerations—e.g., laser power, ratio of the refractive index of the trapped particle and of its surrounding medium, trapped bead size, and bead position in the trap—have to be considered to optimize the use of optical tweezers. Their unique ability to hold and manipulate a *single* particle in a suitable medium without mechanical contact enables exciting new experiments in microrheology [19,20]. Optical tweezers allow studying in detail the interactions between single pairs of colloids with a force resolution on the order of 0.3 pN and nanometer positioning accuracy.

The interaction potential between two colloids in solutions is intensely discussed in the literature [21–32] and re-

mains a challenge for both experiment and theory. Despite its limitations, the Derjaguin-Landau-Verwey-Overbeek (DLVO) theory [21,22] with a repulsive electrostatic and an attractive van der Waals interaction still constitutes the cornerstone in describing the interaction between charged colloids in aqueous salt solutions since more than 50 years. The analytic expression of the repulsive part of the DLVO potential can be obtained by applying approximations to the solution of the Poisson-Boltzmann (PB) equation in planar geometry and employing the Derjaguin approximation (see Sec. III and the Appendix). The applicability of the DLVO theory deteriorates at increasing magnitude of the surface potential and charge due to the linearization and superposition approximation and at increasing counter-ion valence due to the neglect of small-ion correlations.

In the present contribution, we report on measurements of forces between *single* pairs of negatively charged colloids in aqueous salt solutions using optical tweezers. Moreover, our observations are analyzed by using the DLVO theory and solving the Poisson-Boltzmann equation numerically.

II. METHODS AND MATERIAL

Figure 1(a) illustrates the experimental setup, in which one colloid is fixed at the tip of a micropipette and the other one in an optical trap. An inverted microscope (Axiovert S 100 TV, Carl Zeiss, Jena, Germany) was used, and the optical trap was realized with a diode-pumped Nd:YAG laser (1064 nm, 1 W, LCS-DTL 322; Laser 2000, Wessling, Germany), power stabilized to achieve long-term stability. Additionally, the profile of the laser beam was monitored to ensure optimal trapping conditions. After passing an optical isolator, a quarter-wave plate was used to produce circularly polarized light to exclude effects due to reflection differences of the mirrors between the *p* and *s* polarization of the laser light. The beam was expanded and coupled into the back aperture of the microscope objective (Plan-Neofluor 100 × 1.30 Oil, Carl Zeiss, Jena, Germany). Video imaging and the optical position detection were accomplished by a digital camera (KPF 120, Hitachi, Düsseldorf, Germany). The opti-

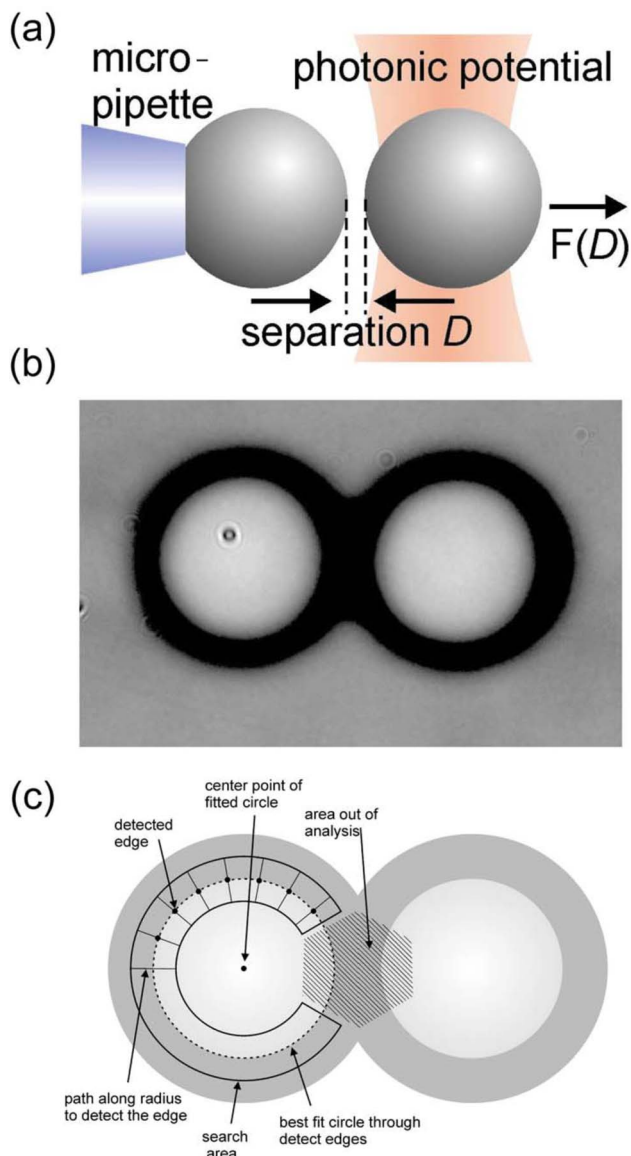


FIG. 1. (Color online) (a) Illustration of the experimental setup, in which the force F at separation D between the solid surfaces of the two negatively charged colloids is measured by using optical tweezers. One colloid is fixed by the tip of a micropipette (blue) and the other in an optical trap established by a photonic potential (brown). (b) Microscope image of the two colloids under study. (c) Illustration of the image analysis algorithm to determine the geometrical center of the two colloids.

cal stage was positioned in three dimensions with nanometer resolution using piezoactuators (P-5173CD, Physik Instrumente, Karlsruhe, Germany). The sample cell consisted of a closed chamber that can be flushed by a syringe pump with varying solutions. A custom-made micropipette with an inner diameter at the tip of $\approx 0.5 \mu\text{m}$ was inserted into the chamber to hold one colloid by capillary action. The whole experimental setup was mounted in a temperature controlled ($298 \pm 1 \text{ K}$) room. The calibration of the optical trap was based on Stokes law as described in detail elsewhere [33,34]. A typical force constant of the trap was 0.085 pN/nm , corresponding to forces in the range between 0.3 and 50 pN ,

which was determined with an accuracy of $\pm 0.3 \text{ pN}$.

The force versus separation dependence $F(D)$ of the interaction between *one single* pair of negatively charged colloids was obtained by image analysis [Fig. 1, panels (b) and (c)]. From the digital images, the displacement of the colloid in the optical trap from the equilibrium position and the separation between the two colloids were determined using a custom-made algorithm with a special edge detection routine in a LabView environment [35,36]. A 60° section, where the two diffraction images overlap [Fig. 1(c)], was removed, and the pathway of the remaining inner edge (given by maximum intensity contrast) was detected and fitted to a circle. The center of the circle defined the position of the center of the colloid. This tracking procedure enabled a reduction of the effects of artifacts in x and y positions to below 2 nm .

Spherical polystyrene beads (microParticles, Berlin, Germany), possessing a negative charge due to surface sulfate groups with $pK_a=1.92$, have been used as colloids. To exclude effects arising from differences among the colloids (variations in diameter, surface roughness, surface charge, etc.), the experiments were performed with *single* pairs of colloids with the surrounding medium changing by flushing the sample cell with salt solutions of different concentration and valency. With this procedure an experiment with a *single* pair of colloids lasted typically $4\text{--}6 \text{ h}$. A measurement sequence comprised $0.3\text{--}30 \text{ mM NaCl}$, $0.15\text{--}3 \text{ mM CaCl}_2$, and $0.003\text{--}0.1 \text{ mM LaCl}_3$ salt solutions at $pH \approx 7.5$. The colloid concentration is below 10^{-18} M , and hence their effect on the ionic strength is negligible. After finalizing the measurement of each valency, the reproducibility of the experiment as a whole was ensured by remeasuring the force-separation dependence in the initial 0.3-mM NaCl solution. At the end of a measurement the average diameter of the two colloids was determined by measuring the force-separation dependence in a 1-M NaCl solution, where the force is well described by a hard-sphere potential (data not shown). For all colloids a diameter of $2.26 \pm 0.02 \mu\text{m}$ was obtained, which was in accordance with light scattering experiments.

III. THEORY

The experimental force-distance data have been analyzed using (i) a size-corrected screened Coulomb interaction and (ii) a numerical approach based on the PB equation in planar geometry augmented with the Derjaguin approximation. The first approach originates from the linearized PB equation in spherical geometry (also referred to as the Debye-Hückel theory). The size-corrected screened Coulomb force is often taken as the electrostatic contribution to the DLVO force acting between two charged colloids (see, e.g., Ref. [1]), but this expression generally differs from the original one given by DLVO [21,22]. In the Appendix we show that the two expressions become the same in a certain limit that approximately holds at the present experimental conditions. The equation proposed by DLVO is only applicable for colloids in symmetric electrolytes; hence, it cannot be used here.

In the screened Coulomb formalism, the electrostatic interaction energy U operating between two equal colloids

possessing the charge Z and radius R at the center-to-center distance r is given by[1]

$$U(r) = \frac{(eZ)^2 \exp[-\kappa(r-2R)]}{4\pi\epsilon_0\epsilon_r (1+\kappa R)^2 r}, \quad (1)$$

where e is the elementary charge, ϵ_0 the permittivity of vacuum, ϵ_r the relative permittivity of the solution, and

$$\kappa = \left[\frac{1}{\epsilon_0\epsilon_r kT} \sum_i (ez_i)^2 c_{i,\text{bulk}} \right]^{1/2} \quad (2)$$

the inverse Debye screening length, with k being Boltzmann constant, T the temperature, z_i the valence of species i , and $c_{i,\text{bulk}}$ the bulk concentration of species i . The interaction energy and the force at surface-to-surface separation $D=r-2R$ become

$$U(D) = \frac{(eZ)^2 \exp(-\kappa D)}{4\pi\epsilon_0\epsilon_r (1+\kappa R)^2 (D+2R)}, \quad (3)$$

and

$$F(D) = \frac{(eZ)^2 \exp(-\kappa D) [1 + \kappa(D+2R)]}{4\pi\epsilon_0\epsilon_r (1+\kappa R)^2 (D+2R)^2}. \quad (4)$$

Since we do not have means to characterize the two colloids individually, we assume their charge and their radius to be equal. The van der Waals attraction also entering in the DLVO interaction can here be neglected, since it contributes only at high salt concentrations (≥ 1 M NaCl) and at surface separations smaller than 10 nm [37–39], in agreement with results from atomic force microscopy [40].

Our numerical PB approach starts with two planar surfaces with the surface charge density σ , which are separated by the distance D and have their normals in the z direction. The intervening medium is in equilibrium with a bulk electrolyte solution. Because of symmetry, only one-half of the system needs to be considered, $0 \leq z \leq b$, $b=D/2$. The amount of ions and their distribution between the two surfaces can be approximated by the PB equation according to

$$\epsilon_0\epsilon_r \frac{d\phi^2(z)}{dz^2} = -e \sum_i z_i c_i(z), \quad (5)$$

where

$$c_i(z) = c_{i,\text{bulk}}(z) \exp[-ez_i\phi(z)/kT], \quad (6)$$

with the boundary conditions

$$\left. \frac{d\phi(z)}{dz} \right|_{z=0} = -\frac{\sigma}{\epsilon_0\epsilon_r}, \quad (7)$$

and

$$\left. \frac{d\phi(z)}{dz} \right|_{z=b} = 0. \quad (8)$$

In Eqs. (5)–(8), $\phi(z)$ is the electrostatic potential at position z relative to the bulk, $c_i(z)$ the bulk concentration of species i at position z , $c_{i,\text{bulk}}$ the concentration of species i in the bulk, and z_i the valence of species i . The numerical solution of Eq. (5)–(8) gives us the potential profile $\phi(z)$ and the

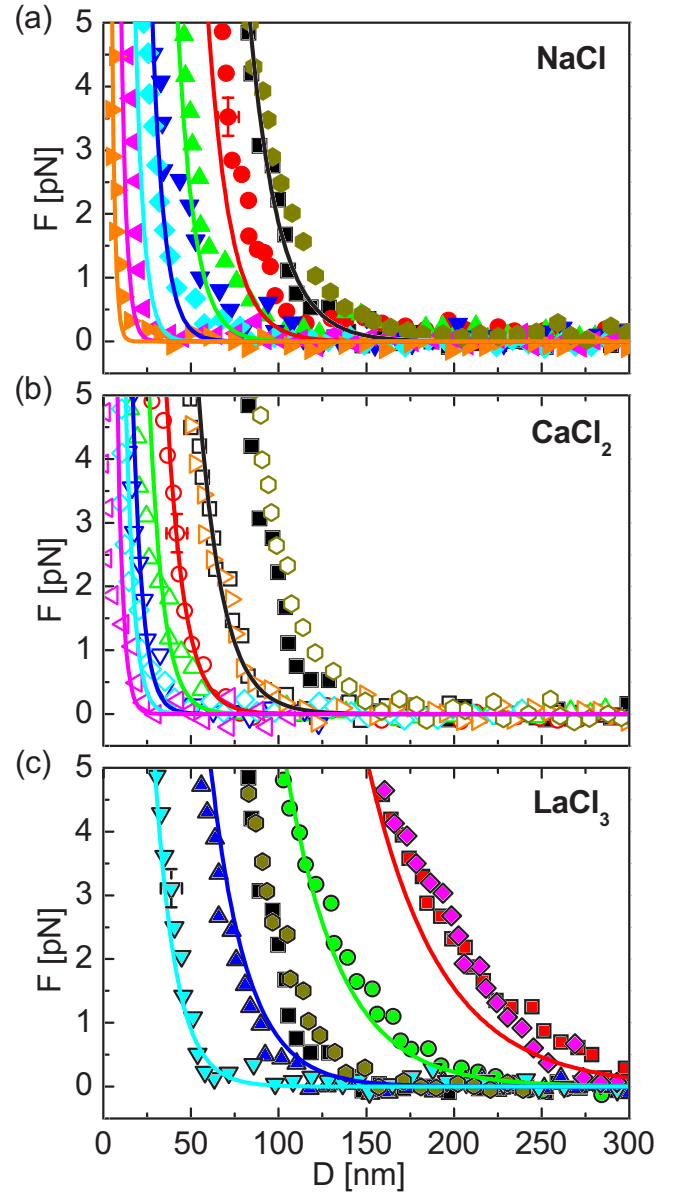


FIG. 2. (Color online) Force F vs separation D for one single pair of colloids in aqueous solution of varying salt and salt concentrations from experiments (symbols) and the DLVO theory with fitted values of the parameters Z and R (curves). (a) NaCl at 0.3 mM (black squares), 0.55 mM (red circles), 1 mM (green triangles), 2 mM (blue nablas), 4 mM (cyan diamonds), 10 mM (magenta left triangles), and 30 mM (orange right triangles). To ensure a full reproducibility of the exchange of the medium and to exclude hysteresis effects due to possible adsorption effects on the colloids the sample cell was flushed again with 0.3 mM NaCl (gold diamonds). (b) CaCl_2 at 0.15 mM (black open squares), 0.3 mM (red open circles); 0.5 mM (green open triangles), 1 mM (blue open nablas), 1.5 mM (cyan open diamonds), 3 mM (magenta open left triangles), 0.15 mM (orange open right triangles), and finally 0.3 mM NaCl (gold open diamonds). (c) LaCl_3 at 3 μM (black red solid square), 10 μM (black green solid circle), 30 μM (black blue solid triangle), 100 μM (black cyan solid nablas), 3 μM (black magenta solid diamonds), and 0.3 mM NaCl solution (black gold solid diamonds). Some indicative error crosses are given.

TABLE I. Fitted colloid charge Z and radius R for three different pairs of colloids in aqueous salt solution with different counterion valence using the DLVO theory [Eq. (1)]. The levels of experimental uncertainties $\sigma^F = \sigma_{\min}^F + 0.25$ pN assuming zero covariance between Z and R are given in brackets. Optimal Z and R values for pair 1 are represented by solid symbols and the covariance between Z and R is demonstrated by the contour lines in Fig. 3.

Colloid pair	Salt	No. of data points	$Z/1000$	R [nm]
1	NaCl	245	218 [156, 267]	1134.6 [1133.0, 1135.4]
	CaCl ₂	108	137 [110, 161]	1131.9 [1130.5, 1132.8]
	LaCl ₃	160	69 [58.9, 79.4]	1135.4 [1131.5, 1138.0]
2	NaCl	266	441 [318, 536]	1135.9 [1133.9, 1136.8]
	CaCl ₂	180	257 [156, 326]	1135.7 [1132.9, 1136.8]
	LaCl ₃	231	66 [42, 82]	1136.9 [1132.6, 1145.0]
3	NaCl	231	283 [203, 346]	1137.1 [1129.0, 1143.3]
	CaCl ₂	174	220 [163, 265]	1138.2 [1136.3, 1139.2]
	LaCl ₃	76	56 [49, 63]	1139.0 [1136.0, 1141.2]

concentration profiles $c_i(z)$ of the species through Eq. (6). The net force F_{plane} per unit area A on a surface can be expressed as the difference in the osmotic pressure in the solution between the surfaces and in the bulk reservoir according to [37]

$$\frac{F_{\text{plane}}}{A} = kT \left[\sum_i c_i(b) - \sum_i c_{i,\text{bulk}} \right], \quad (9)$$

where $c_i(b)$ is the concentration of species i in the midplane. The interaction potential between the two surfaces $U_{\text{plane}}(D)$ is obtained by integrating the force $F_{\text{plane}}(D)$ according to

$$U_{\text{plane}}(D) = - \int_{\infty}^D F_{\text{plane}}(D') dD'. \quad (10)$$

The force between two spherical and charged colloids $F(D)$ at a surface-to-surface separation D is obtained from $U_{\text{plane}}(D)$ by the Derjaguin approximation [21,37] according to

$$F(D) = \pi R \frac{U_{\text{plane}}(D)}{A}, \quad (11)$$

where R is the radius of the colloids. The Derjaguin approximation is valid as long as $D \ll R$, which holds for our colloidal system. Finally, the relation between the surface charge density σ and the colloidal charge Z is given through

$$\sigma = \frac{eZ}{4\pi R^2}. \quad (12)$$

Following the experimental work, $T=298$ K and $\epsilon_r=78.3$ are used throughout in the model calculations.

IV. RESULTS AND DISCUSSION

The experimental force-separation dependences in aqueous salt solution with monovalent (NaCl), divalent (CaCl₂), or trivalent (LaCl₃) counter-ions at varying concentration are displayed in Fig. 2 (symbols). At sufficiently long separation

the force is essentially zero, whereas at decreasing separation the force is monotonously repulsive. The onset of the repulsion appears at shorter separation (i) at increasing salt concentration for a given counter-ion and (ii) at increasing counterion valence at a given salt concentration.

Using the DLVO theory we have made global fits of the colloid charge Z and radius R for three different pairs of colloids using all force curves for a given type of salt by minimizing $\sigma^F = [(1/N) \sum_{i=1}^N (F_i^{\text{calc}} - F_i^{\text{expt}})^2]^{1/2}$, where N is the number of data points, F_i^{calc} the calculated force using Eq. (4), and F_i^{expt} the experimental force. In the case of trivalent counter-ions, the influence of CO₂ in air has to be accounted by assuming 34 μM HCO₃⁻. Table I presents the fitted colloidal charge and radius, and Fig. 2 (curves) displays Eq. (4) with these fitted values. Contour diagrams of σ^F in the Z and R parameter space are shown in Fig. 3. It is seen that the radius is well determined, the uncertainty of the charge is larger, and not surprisingly a considerable covariance appears between Z and R .

Identical global fits but using the PB theory for two charged planes augmented with the Derjaguin approximation for the colloidal pair 1 with monovalent and divalent salt have been made. The obtained colloidal charges and radii were within the 0.25 pN uncertainty domain the same as those obtained using the DLVO theory. It is expected that the fitted charges using the PB theory should be larger than those using the DLVO theory, but this difference is hidden by the relative large uncertainty of the fitted charges.

Figure 4 shows the force versus separation dependence as predicted by the DLVO and PB theories for *same* colloid charge and size. Here we use the optimal Z and R values obtained by fitting the experimental data to the DLVO theory. We notice that the predictions by the DLVO theory agree well with those of the PB theory at the higher salt concentrations, but deteriorate at decreasing salt concentration and are substantial at the lowest salt concentrations at which the magnitude of the surface potential are larger. Obviously, the approximations applied to the PB equation leading to the DLVO theory become noticeable for the present colloidal solution at the lowest salt concentrations considered.

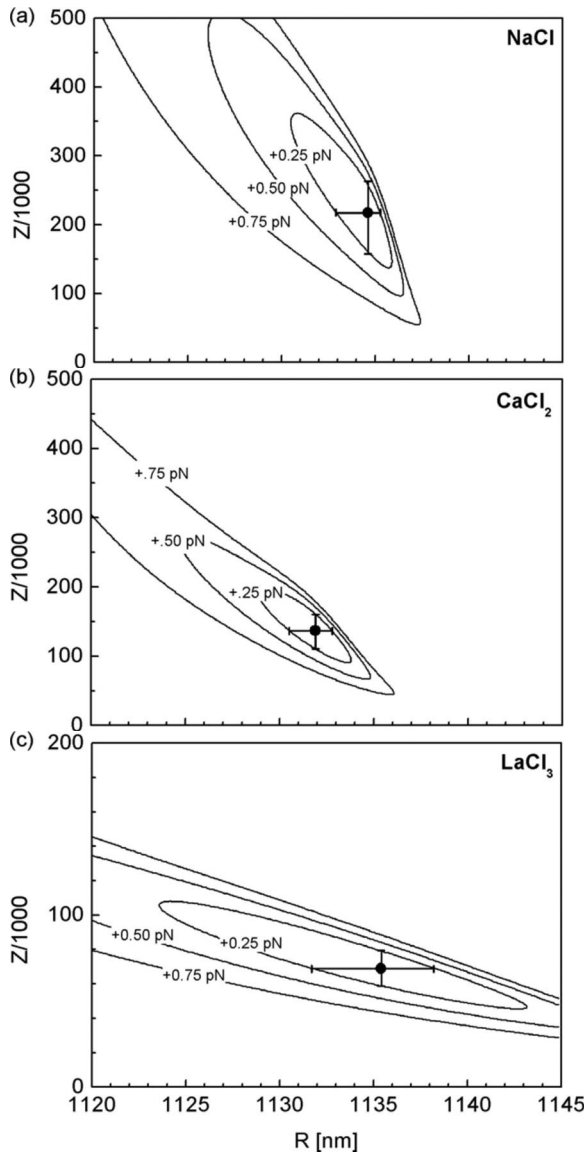


FIG. 3. Contour plots of the root-mean-square deviation σ^F between experimental and predicted [Eq. (1)] force-separation dependences determined at different colloidal charge Z and radius R for (a) NaCl, (b) CaCl₂, and (c) LaCl₃ salt solutions. The locations of the optimal values of Z and R are given (symbols), and corresponding values of σ^F are (a) $\sigma_{\min}^F = 1.28$ pN, (b) $\sigma_{\min}^F = 1.10$ pN, and (c) $\sigma_{\min}^F = 0.40$ pN. The three contour curves represent $\sigma^F = \sigma_{\min}^F + 0.25$ pN, $\sigma_{\min}^F + 0.5$ pN, and $\sigma_{\min}^F + 0.75$ pN, respectively.

Now, (i) the reasonable agreement between the DLVO and PB approaches and (ii) the accumulated experience that the small-ion correlations neglected in both approaches are of minor importance in aqueous solutions with monovalent small ions [39] imply that, except for the lowest salt concentrations, the DLVO theory satisfactorily represents the electrostatic interaction between the colloids in the presence of monovalent salt. Second, a comparison of the fitted Z and R among the three colloidal pairs with monovalent counterions shows that the radii are virtually the same, whereas the fitted charges ranges from $Z \approx 200\,000$ to $450\,000$. Third, for a given pair of colloids, at increasing counter-ion valence the fitted radius R remains essentially constant, whereas the fit-

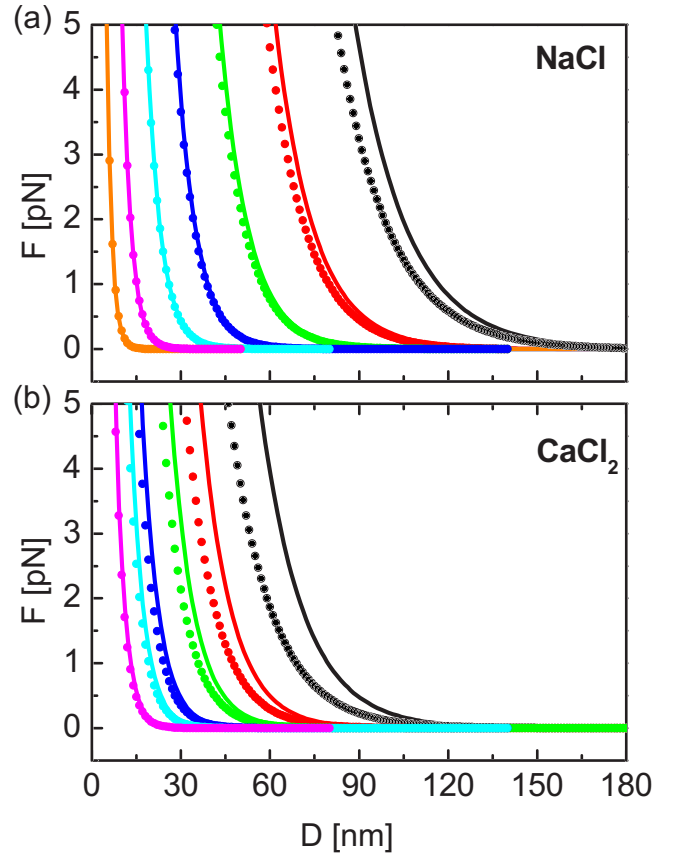


FIG. 4. (Color online) Calculated force F vs separation D for one single pair of colloids in aqueous solution of varying salt and salt concentrations for (a) monovalent counterions at $c_{\text{salt}} = 0.3, 0.55, 1, 2, 4, 10,$ and 30 mM (right to left) with $Z = 218\,000$ and $R = 1134.6$ nm and (b) divalent counterions at $c_{\text{salt}} = 0.15, 0.3, 0.5, 1, 1.5,$ and 3 mM (right to left) with $Z = 137\,000$ and $R = 1131.9$ nm using the DLVO theory (solid curves) and the PB theory (dotted curves).

ted charge Z decreases (Table I). We attribute the latter effect to the neglect of the small-ion correlations in the DLVO theory, which gain importance at increasing counterion valence. The neglect of those leads to an underestimation of screening of the colloids, while the functional force-separation dependence is essentially preserved.

Finally, Fig. 5 displays the surface separation versus the (a) NaCl, (b) CaCl₂, and (c) LaCl₃ concentrations at the specified forces 2 and 4 pN for the three different pairs of colloids as obtained from the experiments and the predictions of the DLVO theory. A similar degree of agreement between the experimental (symbols) and the calculated (lines) as for the force versus distance curves are obtained.

V. CONCLUSION

To conclude, the force-separation dependence for *single* pairs of charged colloids in aqueous solution of monovalent, divalent, or trivalent counterions of varying concentration has been measured using optical tweezers. The results are quantitatively described by the DLVO theory using

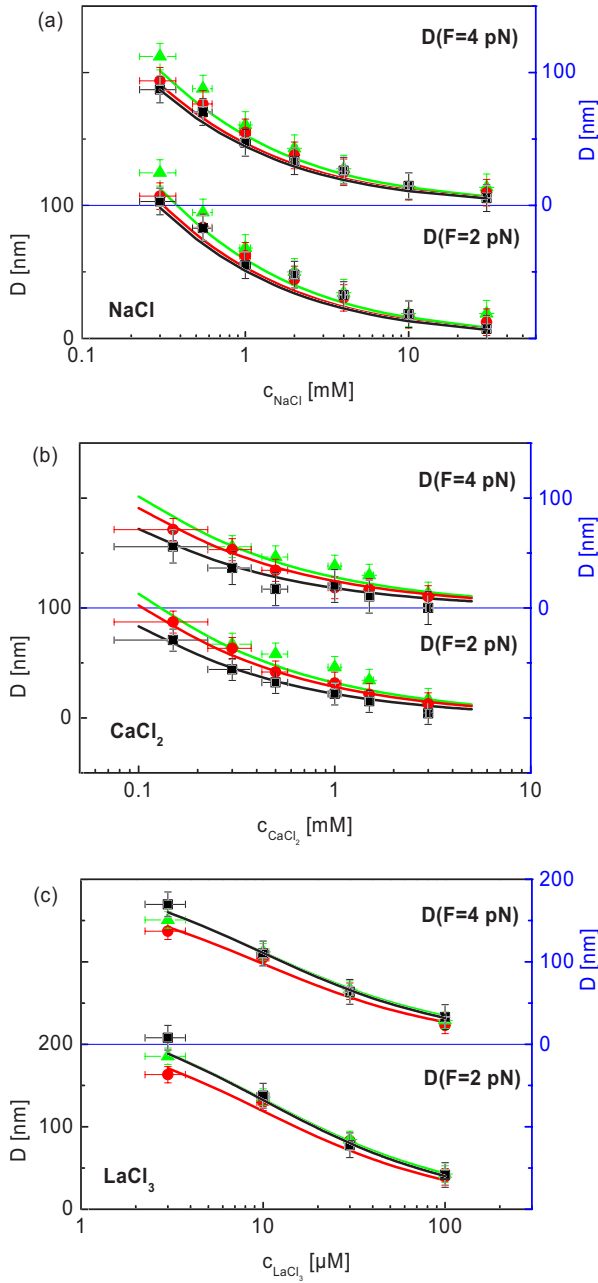


FIG. 5. (Color online) Experimental (symbols) and predicted [Eq. (1), curves with parameters from Table I] surface separation at forces of 2 pN (left ordinate) and 4 pN (right ordinate) vs (a) NaCl concentration, (b) CaCl₂ concentration, and (c) LaCl₃ concentration for colloid pairs 1 (black squares), 2 (green triangles), and 3 (red circles).

concentration-independent effective colloidal charge and stoichiometric Debye screening lengths. However, the resulting effective colloidal charge decreases with increasing counterion valence, which is attributed to the approximations of the DLVO theory.

ACKNOWLEDGMENTS

The authors are indebted to the Institute of Medical Phys-

ics and Biophysics for providing their zetasizer to characterize the colloids. Financial support by the Deutsche Forschungsgemeinschaft within the priority program SPP 1164 on “Nano- and microfluidics” and the Swedish Research Council (VR) is gratefully acknowledged.

APPENDIX

Starting from the PB equation for planar geometry, we will (i) briefly account for the derivation of the electrostatic force according to the DLVO theory and (ii) relate this force with the size-corrected screened Coulomb force [Eq. (4)]. The first part is given in more detail in textbooks; see, e.g., Refs. [37,41,42].

Equation (9) provides the net force between two charged planes immersed in an electrolyte solution. Insertion of Eq. (6) into Eq. (9) and the assumptions of weakly interacting colloids, enabling an expansion of the exponential in Eq. (6) to the second order, give

$$\frac{F_{\text{plane}}}{A} = \frac{1}{2} \varepsilon_0 \varepsilon_r \kappa^2 [\phi(b)]^2. \quad (\text{A1})$$

The next step is to apply the superposition approximation where the electrostatic potential at the mid-plane $\phi(b)$ is approximated according to

$$\phi(b) \approx 2\phi^{\text{GC}}(b), \quad (\text{A2})$$

where $\phi^{\text{GC}}(b)$ denotes the electrostatic potential appearing at the distance b outside a single charged surface in contact with a semi-infinite electrolyte solution. The latter system possesses an analytic solution for symmetric electrolytes (also referred to as the Gouy-Chapman theory). For a $z:z$ electrolyte and sufficiently far from the charged surface such that the electrostatic potential is small, we have

$$\phi^{\text{GC}}(b) = \frac{4kT}{ez} \Gamma_0 \exp(-\kappa b), \quad (\text{A3})$$

where here and in the following z denotes the valence of the $z:z$ electrolyte and Γ_0 is related to the surface charge density σ through the surface potential ϕ_0 according to

$$\Gamma_0 = \tanh\left(\frac{ez\phi_0}{4kT}\right) \quad (\text{A4})$$

and

$$\sigma = (8kTc_{\text{bulk}}\varepsilon_0\varepsilon_r)^{1/2} \sinh\left(\frac{ez\phi_0}{2kT}\right). \quad (\text{A5})$$

Substitution of Eq. (A3) into Eq. (A2) and Eq. (A2) into Eq. (A1) gives

$$\begin{aligned} \frac{F_{\text{plane}}(D)}{A} &= 32\varepsilon_0\varepsilon_r\kappa^2\left(\frac{kT}{ez}\right)^2\Gamma_0^2\exp(-\kappa D) \\ &= 64kTc_{\text{bulk}}\Gamma_0^2\exp(-\kappa D), \end{aligned} \quad (\text{A6})$$

where Eq. (2) has been used. Finally, after integration with respect to D and applying the Derjaguin approximation, we have

$$F(D) = 64\pi RkTc_{\text{bulk}}\Gamma_0^2 \exp(-\kappa D)/\kappa, \quad (\text{A7})$$

which is the electrostatic force acting between two like-charged colloids of the original DLVO theory [21,22,37,41,42].

Our aim is now to examine under conditions at which Eqs. (4) and (A7) are identical. Assume now that the colloids are weakly charged such that Eqs. (A4) and (A5) can be linearized. Thereafter, an elimination of the surface potential ϕ_0 gives the relation

$$\Gamma_0 = \frac{\sigma}{(32kTc_{\text{bulk}}\epsilon_0\epsilon_r)^{1/2}}, \quad (\text{A8})$$

which inserted into Eq. (A7) gives

$$F(D) = 2\pi R \frac{\sigma^2}{\epsilon_0\epsilon_r\kappa} \exp(-\kappa D). \quad (\text{A9})$$

The replacement of the surface charge density σ with the colloid charge Z using Eq. (12) results in

$$F(D) = \frac{1}{2} \frac{(eZ)^2 \exp(-\kappa D)}{4\pi\epsilon_0\epsilon_r \kappa R^3}. \quad (\text{A10})$$

Finally, when the colloid separation is much smaller than their size ($D \ll R$) and the Debye screening length is much smaller than the colloids ($\kappa^{-1} \ll R$), Eq. (4) reduces also to Eq. (A10). To conclude, under the conditions that (i) the linearization can be applied at the surface, (ii) $D \ll R$, and (iii) $\kappa^{-1} \ll R$, Eqs. (4) and (A7) are equivalent. At the present experimental conditions, this is practically the case.

-
- [1] *Ordering and Phase Transitions in Charged Colloids*, edited by A. K. Arora and B. V. R. Tata (VCH, New York, 1996).
- [2] M. E. Leunissen *et al.*, *Nature (London)* **437**, 235 (2005).
- [3] A.-P. Hynninen, M. E. Leunissen, A. van Blaaderen, and M. Dijkstra, *Phys. Rev. Lett.* **96**, 018303 (2006).
- [4] P. I. Kuzmin *et al.*, *Biophys. J.* **98**, 7235 (2001).
- [5] M. Mirza *et al.*, *J. Dispersion Sci. Technol.* **19**, 951 (1998).
- [6] G. Tresset and C. Iliescu, *Appl. Phys. Lett.* **90**, 173901 (2007).
- [7] D. J. Estes *et al.*, *Biophys. J.* **91**, 233 (2006).
- [8] M. B. Fox, *Anal. Bioanal. Chem.* **385**, 474 (2006).
- [9] A. Chonn and P. R. Cullis, *Curr. Opin. Biotechnol.* **6**, 698 (1995).
- [10] A. Ashkin, *Proc. Natl. Acad. Sci. U.S.A.* **94**, 4853 (1997).
- [11] M. Salomo *et al.*, *Colloid Polym. Sci.* **284**, 1325 (2006).
- [12] J. C. Crocker and D. G. Grier, *Phys. Rev. Lett.* **77**, 1897 (1996).
- [13] T. Sugimoto *et al.*, *Langmuir* **13**, 5528 (1997).
- [14] R. Galneder *et al.*, *Biophys. J.* **80**, 2298 (2001).
- [15] U. F. Keyser *et al.*, *Nature (London)* **2**, 473 (2006).
- [16] C. Bustamante *et al.*, *Nature (London)* **421**, 423 (2003).
- [17] A. I. Bishop, T. A. Nieminen, N. R. Heckenberg, and H. Rubinsztein-Dunlop, *Phys. Rev. Lett.* **92**, 198104 (2004).
- [18] M. T. Valentine *et al.*, *J. Phys.: Condens. Matter* **8**, 9477-82 (1996).
- [19] C. Gutsche *et al.*, *Microfluid. Nanofluid.* **2**, 381 (2006).
- [20] N. Garbow *et al.*, *Colloids Surf., A* **195**, 227 (2001).
- [21] B. V. Derjaguin and L. Landau, *Acta Physicochim. URSS* **14**, 633 (1941).
- [22] E. J. Verwey and J. T. G. Overbeek, *Theory of the Stability of Lyophobic Colloids* (Elsevier, Amsterdam, 1948).
- [23] I. Sogami and N. Ise, *J. Chem. Phys.* **81**, 6320 (1984).
- [24] E. Allahyarov, H. Lowen, and S. Trigger, *Phys. Rev. E* **57**, 5818 (1998).
- [25] F. Bitzer, T. Palberg, H. Lowen, R. Simon, and P. Leiderer, *Phys. Rev. E* **50**, 2821 (1994).
- [26] P. Gonza'lez-Mozuelos and M. D. Carbajal-Tinoco, *J. Chem. Phys.* **109**, 11074 (1998).
- [27] P. Maarten Biesheuvel, *Langmuir* **17**, 3553 (2001).
- [28] K. S. Schmitz *et al.*, *Langmuir* **19**, 7160 (2003).
- [29] N. Grønbech-Jensen *et al.*, *Physica A* **261**, 74 (1998).
- [30] H. Löwen and G. Kramppothuber, *Europhys. Lett.* **23**, 673 (1993).
- [31] J. Dobnikar *et al.*, *New J. Phys.* **8**, 277 (2006).
- [32] P. Linse, *J. Chem. Phys.* **94**, 3817 (1991).
- [33] K. Svoboda and S. M. Block, *Annu. Rev. Biophys. Biomol. Struct.* **23**, 247 (1994).
- [34] A. Sischka *et al.*, *Rev. Sci. Instrum.* **74**, 4827 (2003).
- [35] B. Ovryn and S. Izen, *J. Opt. Soc. Am. A* **17**, 1202 (2000).
- [36] B. Ovryn, *Experiment in Fluids* (Springer, Berlin, 2000), pp. 175–184.
- [37] D. F. Evans and H. Wennerström, *The Colloidal Domain where Physics, Chemistry, Biology, and Technology Meet* (VCH, New York, 1999).
- [38] S. N. Thennadil and L. H. G. -Rubio, *J. Colloid Interface Sci.* **243**, 136 (2001).
- [39] R. R. Netz, *Eur. Phys. J. E* **5**, 189 (2001).
- [40] K. Besteman, M. A. G. Zevenbergen, H. A. Heering, and S. G. Lemay, *Phys. Rev. Lett.* **93**, 170802 (2004).
- [41] P. C. Hiemenz, *Principles of Colloid and Surface Chemistry* (Marcel Dekker, New York, 1977).
- [42] J. Israelachvili, *Intermolecular & Surface Forces* (Academic Press, London, 1991).